Journal of Hydroscience and Hydraulic Engineering
Vol. 26, No.2 November, 2008, 1-13

NON-EQUILIBRIUM CHARACTERISTICS OF BAR GEOMETORY ON BED WITH NON-UNIFORM SEDIMENT

By

Hiroshi TAKEBAYASHI

Disaster Prevention Research Institute, Kyoto University
Higashinoguchi, Shimomisu, Yokoouji, Fushimi, Kyoto, JAPAN

And

Shinji EGASHIRA

River Group, Domestic Operational Head Quarter, NEWJEC Inc, 2-3-20 Honjo-Higashi, Kita-ku, Osaka, Japan

SYNOPSIS

Alternate bars on beds with non-uniform sediments are difficult to reach an equilibrium state under some hydraulic conditions. It seems likely that sediment sorting is responsible for the instability of alternate bar bed geometry, because sediment sorting affects local sediment discharge resulting in difference bed geometry. In the present study, the mechanism of the spatiotemporal change of geometric and migration characteristics of alternate bars formed on beds with non-uniform sediment is discussed in terms of numerical analysis and linear bed instability analysis. The results support the notion that alternate bars fail to reach an equilibrium state because of coexist of the same-scaled complex migration velocities.

INTRODUCTION

Previous studies have revealed that the grain size of bed materials should meet certain conditions for spawning of fish and invasion of vegetation (1), (2). Furthermore, even with bed materials of the same mean grain diameter, their different grain size distributions would produce greatly different bed geometries under some hydraulic conditions (3). Therefore, to plan river regulation works for flood control and to create and conserve diversified ecological systems, it is vital to predict quantitatively spatiotemporal changes of both the bed geometry and the grain size of bed materials.

When alternate bars are tried to be formed in a straight experimental flume with a rectangular cross-section, fixed side walls and bed with non-uniform sediment, a phenomenon where the geometric characteristics and migration characteristics of the bars fail to reach an equilibrium state is frequently observed, even though water and sediment are fed constantly. Subsequently, the wave height of the bars decreases with time, and the bars eventually disappear. Normally, it is believed that such a phenomenon is attributable to problems associated with experimental methods. However, alternate bars on beds with uniform sediment, in which the geometric characteristics and migration characteristics reach equilibrium state, are easily obtained in flume experiments. This finding suggests the possibility that temporal changes in geometries of such alternate bars might be a phenomenon that is specific to bed with non-uniform sediment.

Many studies of geometric characteristics and migration characteristics of alternate bars on beds with non-uniform sediment, which are based on flume experiments, theoretical analyses, and numerical analyses, have been performed. Fukuoka, Igarashi, and Kume (4) generated alternate bars in the flume using uniform and non-uniform sediments which have nearly equal mean grain diameter. They investigated regions of bar generation, in addition to differences of geometric characteristics. They found that, with non-uniform sediment, regions of bar generation were observed at a smaller width-depth ratio than those of a uniform sediment bed. Using flume experiments, Miwa and Daido (5), and Takahashi, Egashira, and Yoshizumi (3) investigated differences of equilibrium wave height between alternate bars that were generated on beds with non-uniform and uniform sediment. Their findings showed that the wave height of alternate bars on bed with the non-uniform sediment is lower than that on bed with uniform sediment. Furthermore, Miwa and Daido (5) made detailed measurements of the grain size distribution of bed materials in the bed surface layer and found that sediment sizes at the crest and in the trough tend to be finer and coarser, respectively. Lanzoni (6) and Miwa et al. (7) also performed experiment on bar formation with non-uniform sediment in a straight channel. Then (7) investigated the development and deformation process of bars under unsteady water supply conditions.

Regions of bar generation, geometric and migration characteristics of bars were investigated using linear bed instability analysis, which was almost the same as the method used for a uniform sediment bed. Koyama, Kuroki, and Itakura (8) showed that hydraulic conditions for bar generation on bed with non-uniform sediment are nearly identical to those for bed with uniform sediment except for regions in which the non-dimensional shear stress is small (contents were modified in part by oral presentation made at the conference). Furthermore, Takebayashi (9), and Takebayashi and Egashira (10) made similar linear bed instability analyses conducted by Koyama, Kuroki, and Itakura (8), and showed grain fining at the crest and grain coarsening at the trough. They further showed that the wavelength, wave height, and migration velocity of alternate bars on bed with non-uniform sediment are respectively shorter, lower, and faster than those on bed with uniform sediment. Lanzoni and Tubino (11) made similar linear analyses; the grain size distribution is expressed on a ϕ-scale. According to such analysis (11), different from other experimental and analysis results, the migration velocity of the bar on bed with non-uniform sediment is slower than that on bed with uniform sediment. Furthermore, Hasegawa, Fujita, Meguro, and Tatsuzawa (12) attempted to explain phenomena of bed configurations in the mountainous rivers using a Talbot-type grain size distribution.

Investigations based on numerical analyses have been conducted by Takebayashi, Egashira and Jin (13) and by Takebayashi and Egashira (10). They show that the wavelength, wave height, and migration velocity of alternate bars on beds with non-uniform sediment are, respectively, shorter, lower, and faster than those on bed with uniform sediment. Teramoto and Tsujimoto (14) also made a numerical analysis of the bar formation with non-uniform sediment and discussed the effects of non-uniformity of sediment on the dominant bar mode.

The focus of these studies was on the equilibrium values of geometric characteristics and migration characteristics of bars on beds with non-uniform sediment; in fact, spatiotemporal changes in geometric

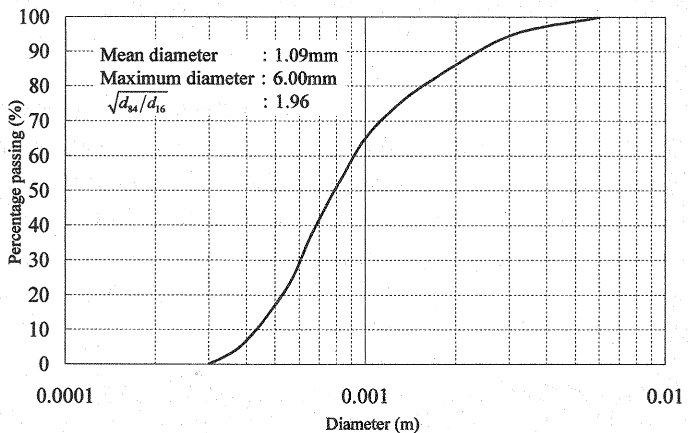

Fig. 1 Size distribution of bed material used in the analysis

characteristics and migration characteristics, in addition to the presence or absence of equilibrium values are not considered. On the other hand, for spatiotemporal changes of geometric characteristics and migration characteristics of alternate bars on bed with non-uniform sediment, Takebayashi and Egashira (15) showed the existence of a phenomenon of bar disappearance. However, sufficient investigations on the bar disappearance have not been made and a problem with treatment of complex migration velocity remains in the theoretical analyses. Consequently, therefore, this study deals with a mechanism for generation of spatiotemporal change of geometric and migration characteristics of alternate bars on bed with non-uniform sediment through numerical analysis and linear bed instability analysis.

NUMERICAL ANALYSIS

Governing equations of the depth integrated two dimensional flow are used to calculate of flows. The flow velocity near the bed is estimated using the streamline curvature of depth averaged flow velocity and the coefficient of the secondary flow intensity employed here is 7.0, which is the same as that used by Engelund (16). Sediment discharge is obtained by using the equations by Ashida, Egashira, and Liu (18), in which influences of the local inclination of the bed on the sediment discharge vector are introduced into the Ashida-Michiue equation (17). To calculate the grain size, the method adopted by Ashida, Egashira, and Liu (18), in which a transition layer is introduced underneath the exchange layer, is used.

The calculation area is a straight flume with fixed side walls (60 m length, 0.3 m width) and a rectangular cross-section. Although the initial shape of the bed is macroscopically flat, the random disturbance which has the amplitude in approximately 1/100 scale of the mean grain diameter is introduced to the entire bed. A constant water discharge is supplied from the upstream boundary. Sediment discharge at the upstream boundary is calculated using equations by Ashida, Egashira, and Liu (18) based on the hydraulic conditions at the boundary. Figure 1 shows bed materials used for analyses. The total number of sediment size class is set to 10. The diameters of each sediment size class are 3.1, 1.9, 1.3, 1.0, 0.85, 0.73, 0.64, 0.57, 0.48, 0.38 (mm). The width-depth ratio is 25; the non-dimensional shear stress with regard to the mean grain diameter is 0.085. The non-dimensional critical shear stress with respect to the mean grain diameter is 0.035. The bed slope used is 1/90. The hydraulic conditions in the numerical analysis are in the formative condition of alternate bars (19).

THEORETICAL ANALYSIS

A linear bed instability analysis is performed on a field that is nearly the same as that used in numerical analyses. However, the terms of turbulence diffusion in the momentum equations of flows are not considered; moreover, the direction of depth integrated water velocity is used for the directions of sediment discharge and shear stress. For the equation of sediment discharge, Meyer-Peter and Müller's equation (20) is used. The difference of the sediment discharge formula between the numerical analysis and the theoretical analysis does not have an effect on the conclusions of this paper. Grain size distributions are calculated only in the exchange layer (21). Dimensionless perturbed variables are given as follows:

$$\left(\tilde{z}_b, \tilde{u}, \tilde{h}, \tilde{d}_m, \tilde{f}_1, \ldots, \tilde{f}_n\right) = \left(\hat{z}_b, \hat{u}, \hat{h}, \hat{d}_m, \hat{f}_1, \ldots, \hat{f}_n\right) e^{ik(\bar{x}-\bar{c}\bar{t})} \cos\left(l\bar{y}\right) \tag{1}$$

$$\tilde{v} = \hat{v} e^{ik(\bar{x}-\bar{c}\bar{t})} \sin(l\bar{y}) \tag{2}$$

In these equations, z_b is the bed elevation, u and v are the depth integrated water velocity in the longitudinal direction and in the traverse direction, respectively. In addition, h denotes the water depth, d_m is the mean grain diameter of bed materials, f_i is the fraction of i sediment size class in the exchange layer, k and l are wave number in the longitudinal direction and in the traverse direction, respectively, and c is the complex migration velocity. Furthermore, ^ denotes the dimensionless amplitude and – denotes the dimensionless quantity. The total number of sediment size class is represented by n. Substituting Eqs. (1) and (2) into linearized and dimensionless governing equations, the following equations are obtained (9).

$$ik\hat{u} + l\hat{v} + ik\hat{h} = 0 \tag{3}$$

$$\left(ikF^2 + 2I\right)\hat{u} + ik\hat{z}_b + \left(ik - I - 2qI\right)\hat{h} - 2qI\hat{d}_m = 0 \tag{4}$$

$$\left(ikF^2 + I\right)\hat{v} - l\hat{z}_b - l\hat{h} = 0 \tag{5}$$

$$-\hat{d}_m + \sum_{i=1}^{n} \bar{d}_i f_{i0} \hat{f}_i = 0 \tag{6}$$

$$\sum_{i=1}^{n} f_{i0} \hat{f}_i = 0 \tag{7}$$

$$2ikA_{si}\alpha_i\hat{u} + lA_{si}\hat{v} + \left(l^2 A_{si}\beta_i - ik\bar{c}\right)\hat{z}_b - 2ikqA_{si}\alpha_i\hat{h} - 2ikqA_{si}\alpha_i\hat{d}_m + \left(-ik\bar{c}\bar{E}_m + ikA_{si}\right)\hat{f}_i = 0 \tag{8}$$

In those equations, $\alpha_i = 1.5\left[\tau_{*i0}/\left(\tau_{*i0} - \tau_{*ci}\right)\right]$, $\beta_i = \sqrt{\tau_{*ci}/\left(\mu_k \mu_s \tau_{*i0}\right)}$, $A_{si} = q_{bi0}/\left[(1-\lambda)u_0 h_0\right]$, $q = 2.5/\left[6.0 + 2.5\ln\left(h_0/d_{m0}\right)\right]$; in addition, F is the Froude number, I is the bed slope, E_m is the thickness of exchange layer, τ_{*i} and τ_{*ci} are the non-dimensional shear stress and non-dimensional critical shear stress of i sediment size class, respectively. Also, μ_k and μ_s are the dynamic friction coefficient and static friction coefficient, respectively, λ denotes the porosity of the sediment. Subscript 0 means the value of the normal flow field. Complex migration velocities are obtained under conditions where the determinant of the coefficient matrix of the simultaneous Eqs. (3)–(8) becomes 0. The interaction among different waves is neglected, because the equations are linearized. Hydraulic conditions used in theoretical analyses are identical to those used in the numerical analysis. The total number of sediment size class is set to 3. The diameters of each sediment size class are 1.9, 0.8, 0.5 (mm).

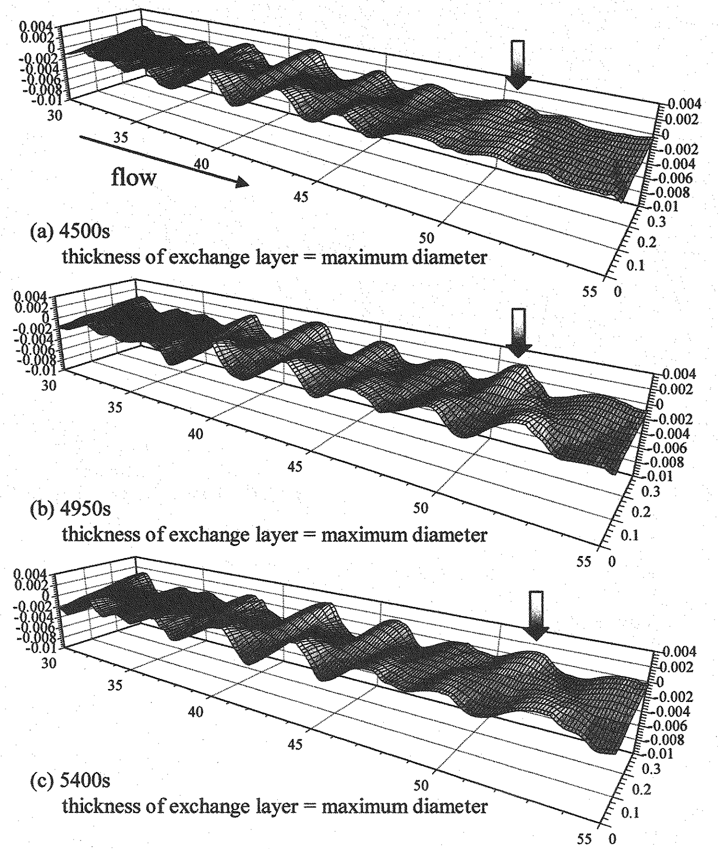

Fig. 2 Decrease process of wave height (Unit: m)

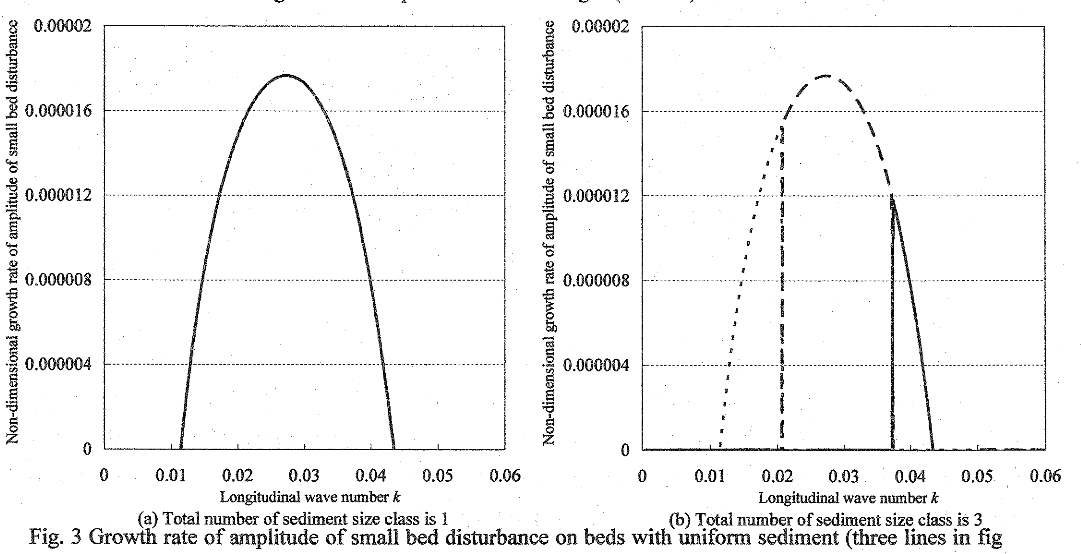

Fig. 3 Growth rate of amplitude of small bed disturbance on beds with uniform sediment (three lines in fig (b) correspond to the growth rate curves of three complex migration velocities)

However, the maximum sediment size which is used to calculate the thickness of exchange layer is the same as that in the numerical analysis.

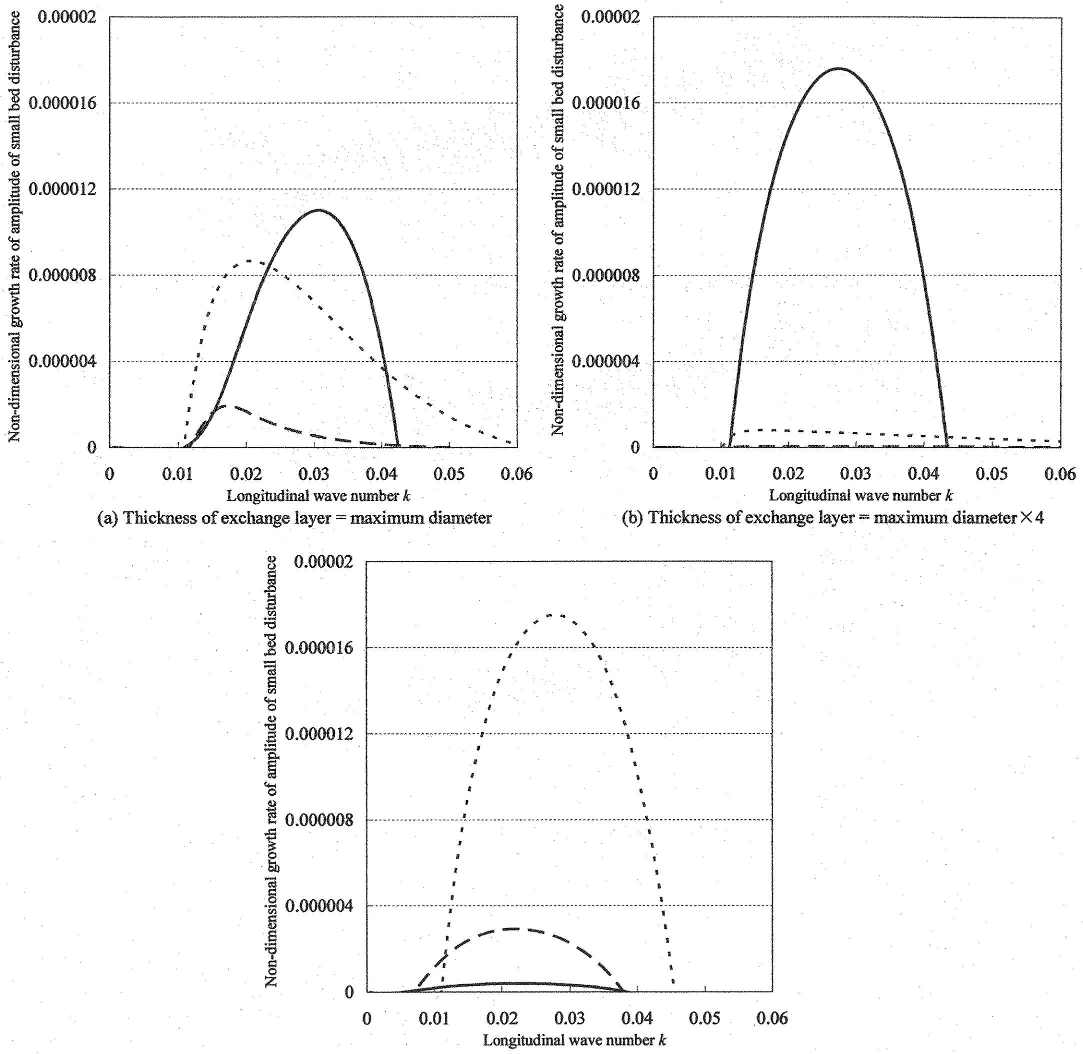

(a) Thickness of exchange layer = maximum diameter

(b) Thickness of exchange layer = maximum diameter × 4

(c) Thickness of exchange layer = maximum diameter ÷ 4

Fig. 4 Effect of thickness of exchange layer on growth rate of amplitude of small bed disturbance

DECREASE OF THE BAR WAVE HEIGHT

Figure 2 shows the process of bar formation by numerical analysis by which the thickness of the exchange layer is used as the maximum grain diameter. The area indicated by the arrow reveals that the wave height of bars being developed up to 4950 s is decreased at 5400 s. Simultaneously, the spatial change of wave height is large. Such a phenomenon is observed by flume experiments (15). On the other hand, this phenomenon does not appear in flume experiments which use bed materials with a narrower grain size distribution.

TREATMENT OF MULTPLLE COMPLEX MIGRATION VELOCITIES

If non-uniform sediments are expressed by dividing them into sediment size classes in the bed instability

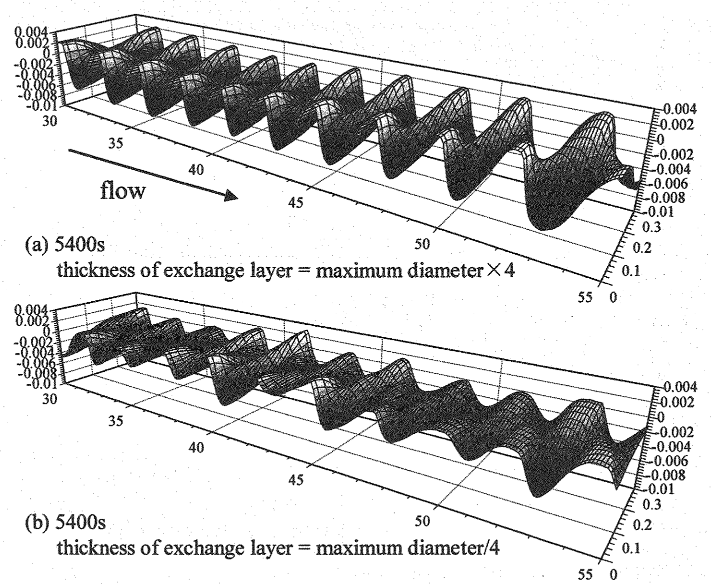

Fig. 5 Effect of thickness of exchange layer on bar geometry (Unit: m)

analysis, complex migration velocities that are the same number of sediment size classes are obtained. The reason for this is that the temporal differentiation of the fraction of each sediment size class is added compared with the analysis using uniform sediments. In other words, when analyses are made with n sediment size classes, complex migration velocities as many as n are obtained as solutions. In general, of these complex migration velocities, the complex migration velocity which has values close to the complex migration velocity on the bed with the uniform sediment are chosen as a complex migration velocity on the bed with the non-uniform sediment (8), (10), (11), (12). Furthermore, one other complex migration velocity is considered as the migration velocity of the sorting wave (11), (12). However, it is not correct to classify these complex migration velocities by variables, because these complex migration velocities are obtained from simultaneous Eqs. (3)–(8) and the forms of solutions are assumed to be those shown by Eqs. (1) and (2). Therefore, the bed, the mean grain diameter and other variables have the same wave number and dimensionless migration velocity. It is reasonable to understand that if n sediment size classes are used, n waves are generated for each variable. To clarify this point, results of linear bed instability analysis done on beds with the uniform sediment are shown in Figure 3. Figure 3 (a) shows the distribution of the growth rate of the bed disturbance with respect to wave number k in the longitudinal direction for the case in which the total number of the sediment size class is 1 and bed materials are treated as uniform sediment. Figure 3 (b) shows similar results for the case in which the total number of sediment size class is 3. All sediment particles are considered to have the same diameter as the uniform sediment, and fractions of each sediment size class are set to 1/3. It is evident from Fig. 3 (b) that three growth rate curves appear because three complex migration velocities are obtained; if their maximum values are combined, it agrees with the result in Fig. 3 (a). That is to say, if any one of the complex migration velocities is only considered as the solution, the instability region might be estimated as small.

RELASHONSHIP BETWEEN THE BED AND THE FRACTIONS OF EACH SEDIMENT SIZE CLASS

Figure 4 (a) shows the distribution of growth rate of bed disturbance with respect to the longitudinal wave

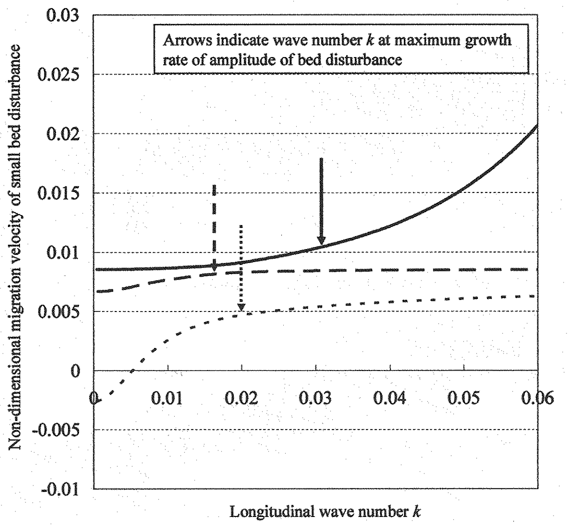

Fig. 6 Difference of migration velocity of small bed disturbance (three lines correspond to the growth rate curves of three complex migration velocities)

number k, which is obtained from the case in which the total number of sediment size classes is 3 and thickness of the exchange layer is equal to the maximum grain diameter. Figure 4 (a) shows that three growth rate curves appear: two have the same scale growth rate, but wave numbers at the maximum growth rates of the two growth rate curves differ greatly. Here, to check the possible relationship of temporal change characteristics between the bed and the fraction of each sediment size class, the exchange layer thickness is changed. Although future investigations are necessary for the appropriate thickness of exchange layer, the maximum grain diameter is used as a reference: four times and 1/4 of this are used in this study. Here, the thickness of the thin exchange layer is thinner than the maximum diameter. However, there is no theoretical problem, because the phenomena are treated as continuum model. Figure 4 (b) shows the case in which the exchange layer thickness is as four times as the maximum grain diameter. Because changes in the grain size become slower and sediment sorting development is delayed, if the exchange layer thickness is thickened, it is anticipated that results might approach those of the uniform sediments. One can see from Fig. 4 (b) that only one growth rate curve became large: the other became small. Furthermore, the growth rate curve enlarged comes close to the growth rate curve of uniform sediment. On the other hand, Fig. 4 (c) shows the case in which the thickness of the exchange layer is 1/4 of the maximum grain diameter. Changes in the grain size become greater and faster, if the thickness of the exchange layer becomes thinner. Similarly, only one growth rate curve becomes large; the other becomes small. However, it does not come close to the growth rate curve on bed with uniform sediment. Figure 5 shows results of the numerical analysis. In Fig. 5 (a), we can observe that if the exchange layer is thickened, remarkably periodic bars are reproduced. This almost agrees with results of the analysis, in which bed materials are considered as uniform sediment. In contrast, we can observe in Fig. 5 (b) that if the thickness of the exchange layer is thinned, the wave height becomes higher than the case in which the exchange layer thickness is assumed to be the maximum grain diameter and geometry of alternate bars are well-defined. Under these conditions, there is no case in which bars disappear and the bed becomes flat. Figure 6 shows migration velocities for the case in which the exchange layer thickness obtained by means of linear analysis is used as the maximum grain diameter. Three migration velocities differ in their values; if they were to be generated simultaneously and bars were observed with the moving coordinate system of a velocity that is the same as either migration velocity, temporal changes in bar

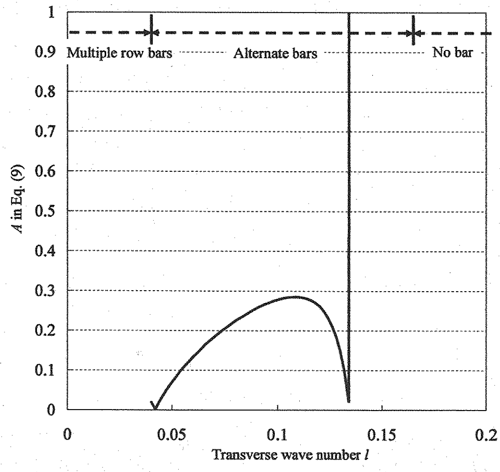

Fig. 7 Relationship between maximum growth rates of two largest growth rate curves

geometry would appear. The above discussions imply that spatiotemporal change of geometric and migration characteristics of alternate bars on beds with the non-uniform sediment are determined by a comparative relationship between temporal changes in the bed and temporal changes in fractions of each sediment size class; they occur when there exists a number of growth rate curves with the same scale, as shown in Fig. 4 (a). Furthermore, because it is believed that the interference between disturbances is smaller under the condition in which the difference of wave numbers at the maximum growth rate is large, the difference of wave number k is also considered important.

Moreover, as shown in Figs. 4 (a) and 4 (c), the maximum growth rate of the growth rate curve increases, when the thickness of the exchange layer becomes thinner. According to the results obtained by using the numerical analysis shown in Fig. 2 and Fig. 5 (b), the space averaged wave height for the case in which the exchange layer thickness is equal to the maximum grain diameter is lower, which agrees with the results of the linear analyses. The results thus suggest that the development of sediment sorting phenomenon does not necessarily suppress the wave height.

GENERATION REGION OF ALTERNATE BARS ON BED WITH NON-UNIFORM SEDIMENT

Figure 7 shows the distribution of values calculated using the following Eq. (9) for traverse wave number l.

$$A=(a_1-a_2)/a_1 \tag{9}$$

In that equation, a_1 represents the maximum growth rate among all growth rate curves, a_2 is the maximum growth rate among growth curves not including a_1. Here, a_1 and a_2 are positive; if they are less than 0, A is represented as greater than 1. In short, when this value is 1, only one growth rate curve is distinguished; when this value is 0, two growth rate curves (both having identical maximum growth rates) exist. The total number of sediment size class is 3 and the thickness of the exchange layer is equal to the maximum sediment diameter. It can be observed from Fig. 7 that the growth rate is less than 0.3 over the entire region of alternate bar generation except for the proximity of the boundary between the alternate bar generation region and the no bar region, which suggests that more than two growth rate curves with the same scale exist in the region of alternate bar generation. Furthermore, the value of A becomes 0 near the boundary between the multiple row bars and alternate bars and around l = 0.134; two growth rate curves with identical maximum growth rates exist at these two wave numbers. Consequently, there is a possibility that two bed

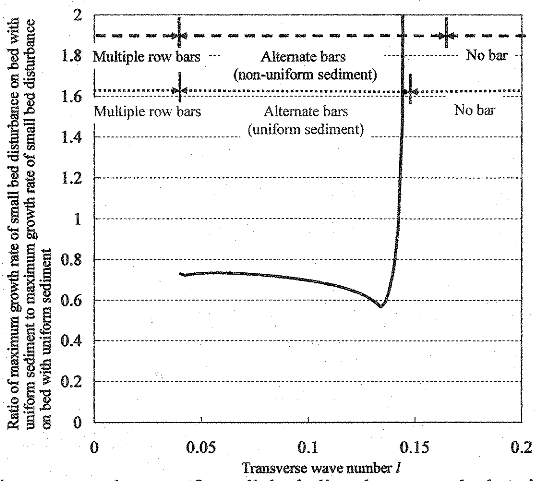

Fig. 8 Ratio of maximum growth rate of small bed disturbance on beds with uniform sediment to maximum growth rate of small bed disturbance on beds with uniform sediment

disturbances grow with the same growth rate and coexist. Here, wave numbers k at the maximum growth rate of these two growth rate curves have different values. Although a difference exists between two maximum growth rates under the condition in Fig. 4 (a), it is believed that because this difference is less and wave numbers between them is greatly different, both bed disturbances grow and coexist.

Figure 8 shows a distribution of the ratio of the maximum growth rate of disturbances on bed with the uniform sediment to the maximum growth rate of disturbances on bed with the non-uniform sediment with respect to wave number l. In Fig. 8, the bar generation regions on beds with the uniform sediment and on beds with the non-uniform sediment are shown together. A comparison of alternate bar generation regions in both beds indicates that although the boundary of generation of multiple row bars and of alternate bars are identical, the boundary of generation of alternate bars and of no bar shift toward the no bar region in the non-uniform sediment bed. This is in line with findings by Fukuoka, Igarashi, and Kume (4). The ratio of the maximum growth rates is less than 1 in a broad range of the alternate bar generation region, which agrees with the fact that the wave height of bars on beds with the non-uniform sediment is lower than that on beds with the uniform sediment. However, the physical meaning of this value is less significant under conditions in which the geometric and migration characteristics of the bars change spatiotemporally. On the other hand, the growth rate of bed disturbance on beds with the non-uniform sediment is greater than that on beds with uniform sediment, because the bar generation region might be expanded in the non-uniform sediment bed around the boundary between the alternate bar and the no bar.

CONCLUSION

This study has examined a mechanism for generation of spatiotemporal change of geometric and migration characteristics of alternate bars on bed with non-uniform sediment through numerical analysis and linear bed instability analysis. Findings obtained in the present study can be summarized as follows:

(1) There exists a condition under which bars (the geometric and migration characteristics of which vary with time) are formed on beds with the non-uniform sediment.

(2) It is thought that temporal changes of geometric and migration characteristics of alternate bars on beds with the non-uniform sediment are determined according to a comparative relationship between temporal changes in the bed

and temporal changes in fraction of each sediment size class. They occur when there are complex migration velocities which have growth rate curves of the same scale.

(3) A possibility exists that more than two growth rate curves with identical scale exist in the bar generation region, and that a number of bed disturbances grow and coexist.

(4) A comparison of an alternate bar generation region between a uniform sediment bed and a non-uniform sediment bed reveals that the boundary between alternate bar generation and no bar shifts toward the no bar region.

(5) In a broad range of the alternate bar generation region, the maximum growth rate of disturbances on beds with the non-uniform sediment is smaller than that on beds with the uniform sediment, which agrees with the fact that the wave height of bars on beds with the non-uniform sediments is lower than that on beds with uniform sediments. On the other hand, around the boundary between alternate bars and the no bar regions, the growth rate of bed disturbances on bed with the non-uniform sediments becomes greater than that on beds with uniform sediments.

ACKNOWLEDGMENTS

This work is funded by Grant-in-Aid for Scientific Research (B) (Representative: Yasuyuki Shimizu) and Grant-in-Aid for Scientific Research for young researchers (B) (Representative: H. Takebayashi). It is mentioned herein and deeply appreciated by the authors.

REFERENCES

1. Kamada, M., Kohri, M., Mihara, S. and Okabe, T.: Distribution of Salix Spp. and Elaeagnus Umbellata communities in relation to their stand characteristics on bars in Yoshino River, Shikoku, Japan, Environmental Systems Research, Vol.27, pp.331-337, 1999.2
2. Tamai, N. Mizuno, N. and Nakamura, S.: River Ecological Engineering, University of Tokyo Press, pp. 89-95, 1993.
3. Takahashi, F., Egashira S. and Yoshizumi, M.: Effect of non-uniform sediment on geometric characteristics of bars, Kansai Chapter Proc. of Annual Conference of Civil Engineers, JSCE, II-68, 1995.
4. Fukuoka, S., Iagrashi, T. and Kume, M.: Transformation process of bed forms under unsteady flow, Annual Journal of Hy. Eng. JSCE, Vol. 29, pp.479-484, 1985.
5. Miwa, H. and Daido, A.: Geometric characteristics of alternate bars and sediment sorting on bed with non-uniform sediment, Kansai Chapter Proc. of Annual Conference of Civil Engineers, JSCE, II-59, 1995.
6. Lanzoni, S.: Experimental on bar formation in a straight flume -2. Graded sediment-, Water Resources Research, Vol. 36, No. 11, pp. 3351-3363, 2000.
7. Miwa, H., Daido, A. and Yokogawa, J.: Development and transformation of alternate bars under unsteady flow, Annual Journal of Hy. Eng. JSCE, Vol. 47, pp. 619-624, 2003.
8. Koyama, S., Kuroki, M. and Itakura, T.: Theoretical study on alluvial bar with non-uniform sediment, Proc. of Annual Conference of Civil Engineers, JSCE, Vol.53, No.2, pp.450-451, 1998.
9. Takebayashi, H: Sediment hydraulic research on bars formed in straight channel, Doctor Engineer thesis, Ritsumeikan University, pp. 45-78, 1999.
10. Takebayashi, H., and Egashira, S.: Dynamic state of sand bar formed on non-uniform sediment bed, Annual Journal of Hy. Eng. JSCE, Vol.45, pp. 727-732, 2001.

11. Lanzoni, S. and Tubino, M.: Grain sorting and bar instability, J. Fluid Mech, vol. 393, pp. 149-174, 1999.
12. Hasegawa, K., Fujita, T., Meguro, H. and Tatsuzawa, H.: Bed forms in steep channels with heterogeneous bed materials induced by bottom elevation instability and sorting instability, Annual Journal of Hy. Eng. JSCE, Vol.44, pp. 659-664, 2000.
13. Takebayashi, H., Egashira S. and Jin, H. S.: Numerical simulation of alternate bar formation, Proc. of 7th ISRS, pp.733-738, 1998.
14. Teramoto, A., and Tsujimoto, T.: Effect of bed-materials composition on mechanism to determine bar mode, Annual Journal of Hy. Eng. JSCE, Vol. 48, pp. 1003-1008, 2004.
15. Takebayashi, H. and Egashira, S. : Instability of developed alternate bar on non-uniform sediment bed, XXIX IAHR Congress Proceedings, Theme D, Tsinghua University Press, Vol. II, ISBN 7 302 04676 X, pp.362-368, 2001.
16. Engelund, F. : Flow and Bed Topography in Channel Bends, Jour. of Hy. Div. ASCE, Vol. 100, No. HY11, 1974.
17. Ashida, K. and Michiue, M.: An investigation of river bed degradation downstream of a dam, Proceedings of 14th Congress of the IAHR, 1971.
18. Ashida, K., Egashira, S. and Liu, B. Y.: Numerical method on sediment sorting and bed variation in meander channels, Annual Journal of Hy. Eng. JSCE, Vol. 35, pp. 383-390, 1991.
19. Kuroki, M. and Kishi, T.: Study on regime criteria of river morphology, Annual Journal of Hy. Eng. JSCE, Vol. 26, pp. 51-56, 1982.
20. Meyer-Peter, E. and Müller, R. : Formulas for bed-load transport, Proc. 2nd IAHR Meeting, pp. 39-64, 1948.
21. Hirano, M.: Studies on variation and equilibrium state of a river composed of nonuniform material, Proc. of JSCE, No. 207, pp. 51-60, 1972.

APPENDIX – NOTATION

The following symbols are used in this paper:

c	= complex migration velocity;
d_m	= mean grain diameter of bed materials;
E_m	= thickness of exchange layer;
F	= Froude number;
f_i	= the fraction of i sediment size class in the exchange layer;
h	= water depth;
I	= bed slope;
$k\ (=\pi h_0/L)$	= wave number in longitudinal direction;
$l\ (=\pi h_0/B)$	= wave number in traverse direction;
n	= total number of size classes of bed material;
u, v	= depth integrated water velocity in the longitudinal direction and in the traverse direction, respectively;
z_b	= bed elevation;
λ	= porosity of the sediment;
μ_k	= coefficient of dynamic friction;
μ_s	= coefficient of static friction;

τ_{*ci}	= non-dimensional critical shear stress of sediment size class *i*;
τ_{*i}	= non-dimensional shear stress of sediment size class *i*;
^	= non-dimensional amplitude of perturbation;
-	= non-dimensional value; and
subscript 0	= value of the normal flow field.

(Received Jun 29, 2007 ; revised Aug 21, 2008)